GENERAL SOURCE AND RECEIVER POSITIONS IN COARSE-GRID FINITE-DIFFERENCE SCHEMES

RUNE MITTET[1] and BØRGE ARNTSEN[2]

[1] *Sting Research, Rosenborg gt. 17, N-7014 Trondheim, Norway.*
[2] *Statoil Research Centre, Postuttak, N-7005 Trondheim, Norway.*

(Received October 29, 1999; revised version accepted March 10, 2000)

ABSTRACT

Mittet, R. and Arntsen, B., 2000. General source and receiver positions in coarse-grid finite-difference schemes. *Journal of Seismic Exploration*, 9: 73-92.

Coarse grid finite-difference schemes do not allow for general source and receiver positions. This problem is here solved with optimized operators with general phase-shift properties. These operators are bandlimited representations of the Dirac delta function and the derivative of the Dirac delta function. The scheme is tested for a single source and a source array. The resulting finite-difference solutions are for both cases close to the analytical solution.

KEY WORDS: modeling, finite-difference, staggered-grid, marine source array, phase-shift interpolation, coarse-grid.

INTRODUCTION

Coarse-grid methods like pseudo-spectral methods (Fornberg, 1975; Kosloff and Baysal, 1982) or high-order finite-difference methods (Holberg, 1987) are ideally suited for implementing fast and memory efficient 3-D elastic modeling schemes (Mittet et al., 1988; Reshef et al., 1988). These methods require few nodes per shortest wavelength in order to describe a propagating wavefield, thus both storage requirements and the number of numerical calculations are reduced as compared to low order finite-difference schemes.

However, there are problems implementing the source function when the typical distance between adjacent grid points is of the order of 10 m. Even a single airgun can not be correctly implemented, unless the true source depth coincide with a grid node. Assuming a grid spacing of 10 m, then the source must be placed at the depth of 10 m since there are no nodes between the free surface and this depth. If the true depth of the source is 4 m, then the ghost contribution cannot be properly described using a coarse grid. The problem is even larger if a marine source array is to be simulated. A conventional marine source array consists of a number (from 5 to 70) of individual air guns, typically separated by 1 - 4 m. This implies that effective point-source signatures estimated from measurements cannot be implemented directly in a coarse-grid finite-difference scheme. This problem was solved in Landrø et al. (1993) by using an inversion scheme prior to the finite-difference modeling, generating effective sources at chosen node positions. In this paper we present a method which obviates this inversion based preprocessing of the source contribution and include the source contribution directly at the true depth, independently of the grid spacing. The new scheme also allows for arbitrary receiver positions. The method is based on generating optimized bandlimited approximations to the Dirac delta function and its first derivative, where these bandlimited functions are designed with a general phase shift. The resulting operators represent a generalization of the operators given by Holberg (1987).

Ziolkowski et al. (1982) presented a method for determining the source wavefield from near-field measurements of the signature of each gun in a marine source array. Landrø and Sollie (1992) and Amundsen (1993) have given alternative methods for determining effective sources. By using the proposed optimized bandlimited delta-function operators these effective source contributions can be included directly at an arbitrary position in a coarse grid finite-difference scheme.

Other applications of these operators are in reverse time migration where a spatially non-regularly sampled boundary condition can be included on a regularly spaced grid and in data recording where output can be performed at an arbitrary position. The implementation of the elastic Kirchhoff integral for finite-difference schemes is discussed in Mittet (1994). The spatial part of the boundary condition requires a description of the monopole operator (Dirac delta function) and the dipole operator (derivative of Dirac delta function). Zhu and Lines (1997) point out that the seismic wavefield has a capability of "healing itself" during retropropagation and due to this, interpolation as a preprocessing step to the reverse time migration may be avoided. For spatially non-regularly sampled data, the contributions to the boundary condition should be introduced at the true positions, not at the nearest node positions of the finite-difference grid. This is possible with the proposed optimized phase-shifted operators. The

required wavenumber limits, then the response at any location can be calculated using the optimized convolutional interpolation operator. Simulating a real experiment, group summation can be performed during modeling and in addition a streamer with variable depth and feathering may be simulated.

Introducing the source at an undesired depth causes both a distortion of the waveform and an erroneous radiation pattern. The error in source amplitude as a function of radiation angle is frequency dependent and can be fairly large. We discuss this after the theory section. We also give results for a realistic source array where the effective source signatures (notional source signatures) are known. Finally we give an example with a streamer having a variable depth. The standard procedure of recording at the nearest nodes is compared with the scheme of recording at the true positions.

THEORY

For simplicity we discuss the implementation of the optimized phase-shift source and receiver operators using the 3D acoustic wave equation, but the operators can be implemented directly in a 3D staggered-grid elastic finite-difference scheme. In the following, the Einstein summation convention is used. The acoustic wave equation for forward modeling with a source signature S(t) is,

$$\partial_t^2 P(\mathbf{x},t|\mathbf{x}_s) - M(\mathbf{x})\partial_j\{\rho^{-1}(\mathbf{x})\partial_j P(\mathbf{x},t|\mathbf{x}_s)\} = \delta(\mathbf{x}-\mathbf{x}_s)S(t) \quad , \tag{1}$$

where $P(\mathbf{x},t|\mathbf{x}_s)$ is the pressure due to a source at $\mathbf{x}_s$, $\rho(\mathbf{x},t)$ is the density and $M(\mathbf{x})$ is the bulk modulus. The pressure field is identically zero before the source is fired. The acoustic wave equation for retropropagation used in reverse time migration is,

$$\partial_t^2 P(\mathbf{x},t|\mathbf{x}_s) - M(\mathbf{x})\partial_j\{\rho^{-1}(\mathbf{x})\partial_j P(\mathbf{x},t|\mathbf{x}_s)\}$$

$$= \oint_A dA(\mathbf{x}_r)\rho(\mathbf{x}_r)^{-1}n_i[\delta(\mathbf{x}-\mathbf{x}_r)\partial_i^r P(\mathbf{x}_r,t) + \partial_i\delta(\mathbf{x}-\mathbf{x}_r)P(\mathbf{x}_r,t)] \quad , \tag{2}$$

where n_i is a surface normal and the surface integral is implemented as a sum over receiver positions weighted with the corresponding surface area elements. If the receiver positions do not coincide with the nodes of the grid, then bandlimited approximations with general phase-shift properties to the Dirac delta function and the derivative of the Dirac delta function are required. Equation (2) is a representation of the well known Kirchhoff integral. The formal final condition at time t = T is that the pressure field and its spatial derivatives must

towards t = 0. The normal situation is that the pressure field is not known on a closed surface, this will introduce aperture effects.

Equation (1) or equation (2) can be solved by the same high-order finite-difference scheme as shown in Mittet (1994). The discrete derivative operator is given in equation (A-3). The staggered-grid implementation requires two special cases of the operator coefficients α_l^η. These special cases are the forward derivative operator coefficients $\alpha_l^{0.5}$ and the backward derivative operator $\alpha_l^{-0.5}$. Here η gives the shift $\delta x = \eta \Delta x$ from a node. With $-0.5 \leq \eta \leq 0.5$ all locations between nodes can be accessed. For a general shift $\eta \Delta x$ the operator has an odd number of coefficients, but for $\eta = 0.5$ and $\eta = -0.5$ one of the coefficients ($l = -L$ or $l = L$, respectively) is zero and the operator coefficients are anti symmetric with respect to the index l. The set of operator coefficients $[\alpha_l^{0.5}]$ are identical to the set of operator coefficients $[\alpha_l^{-0.5}]$ except for a shift of one position. As an example, let L = 2, if

$$[\alpha_{L=2}^{0.5}] = (0, -\alpha_2, -\alpha_1, \alpha_1, \alpha_2) \ ,$$

then

$$[\alpha_{L=2}^{-0.5}] = (-\alpha_2, -\alpha_1, \alpha_1, \alpha_2, 0) \ .$$

With α_l the coefficients of $[\alpha_l^{0.5}]$, the forward derivative in the i-direction can be expressed as (Holberg, 1987)

$$\partial_i^+ \phi_j = (1/\Delta x_i) \sum_{l=1}^{L} \alpha_l (\phi_{j+l} - \phi_{j-l+1}) \ ,$$

and the backward derivative in the i-direction can be expressed as

$$\partial_i^- \phi_j = (1/\Delta x_i) \sum_{l=1}^{L} \alpha_l (\phi_{j+l-1} - \phi_{j-l}) \ .$$

With these operators, a staggered-grid high-order modeling scheme can implemented. Let x = iΔx, y = jΔy, z = kΔz and t = nΔt,

$$\begin{aligned} A_{i+\frac{1}{2},j,k} &= \rho^{-1}_{i+\frac{1}{2},j,k} \partial_x^+ P^n_{i,j,k} \ , \\ B_{i,j+\frac{1}{2},k} &= \rho^{-1}_{i,j+\frac{1}{2},k} \partial_y^+ P^n_{i,j,k} \ , \\ C_{i,j,k+\frac{1}{2}} &= \rho^{-1}_{i,j,k+\frac{1}{2}} \partial_z^+ P^n_{i,j,k} \ , \end{aligned} \tag{3}$$

and

$$U_{i,j,k} = M_{i,j,k} \partial_x^- A_{i+\frac{1}{2},j,k} \ ,$$

$$V_{i,j,k} = M_{i,j,k} \partial_y^- B_{i,j+\frac{1}{2},k} \ ,$$

then a second-order time integration of the scheme gives

$$P^{n+1}_{i,j,k} = 2P^{n}_{i,j,k} - P^{n-1}_{i,j,k} + U_{i,j,k} + V_{i,j,k} + W_{i,j,k} + D_{I,J,K}S^{n} \quad , \tag{5}$$

where D is the spatial part of the source term. This term is a bandlimited approximation to the 3D Dirac delta function,

$$\delta(\mathbf{x}-\mathbf{x}_s) = \delta(x-x_s)\delta(y-y_s)\delta(z-z_s) \quad , \tag{6}$$

and can be constructed from the coefficients β^{η}_{l} given in appendix B. The capital index $I(i,i_s,\eta_s)$ depends on i,i_s,η_s so that,

$$x = i\Delta x \quad , \quad x_s = (i_s + \eta_s)\Delta x \quad , \tag{7}$$

and likewise for the capital indices J and K.

This implies that S^n, the contribution from the temporal source term at time $n\Delta t$, is in principle distributed over several nodes in all spatial directions and such that this three-dimensional bandlimited delta-function approximation is centered at the true source position $\mathbf{x}_s$ and not at the nearest node. The coefficients of $D_{I,J,K}$ are such that if $\mathbf{x}_s$ coincides with a node position, then

$$D_{I,J,K} = (1/\Delta x)(1/\Delta y)(1/\Delta z) \quad ,$$

for $i = i_s$, $j = j_s$ and $k = k_s$ and zero otherwise.

For recording purposes a direct 3D generalization of equation (B-3) can be used,

$$\begin{aligned} P^{n}(x_r,y_r,z_r) &= B^{\eta x}_{x} B^{\eta y}_{y} B^{\eta z}_{z} P_{i,j,k} \\ &= \sum_{l_x=-L_x}^{L_x} \sum_{l_y=-L_y}^{L_y} \sum_{l_z=-L_z}^{L_z} \beta^{\eta x}_{lx}\beta^{\eta y}_{ly}\beta^{\eta z}_{lz} P_{i+l_x,j+l_y,k+l_z} \quad . \end{aligned} \tag{9}$$

The operator half lengths L_{x_i} are usually of order 10 to ensure high numerical precision for all phase shifts. The computer time needed to perform this triple sum is normally small compared to the computer time needed to step the wavefield forward in time since the number of receivers usually is much less than the total number of grid nodes and recording is not necessary at each time step in order to sample the field properly.

The operators for both sources and receivers take the form of 2D tables. Each source or receiver position has nearest node coordinates for each spatial

length 2L + 1 for each η-value. The η-discretization can be made arbitrarily fine since the table has to be built only once.

The normal situation is that sources are close to the top edge of the grid. The source operator can be fairly long and may formally reach far above the top free surface. However, this can be treated consistently. Our assumption is that there is vacuum outside the grid, and hence, the pressure field is identically zero here. Starting sound propagation in vacuum is not possible, so numerically we sum over all operator coefficients inside grid boundaries only, the contribution from those outside the grid boundaries must be zero.

NUMERICAL EXAMPLE

The first example is for a single source located at a true depth of 4 m. The recording is performed at a depth of 100 m. The finite-difference node spacing is 10 m. The P-wave velocity is 1480 m/s and the density is 1.0 g/cm^3. The results are shown in Figs. 1 and 2. Fig. 2 show a detail of Fig. 1. The analytical solution is plotted with a green line. The red line is the result of a finite-difference simulation where the source is assumed to be located at the nearest node. The optimized spatial delta functions are not used in this simulation. Thus, in the finite-difference simulation the source depth becomes 10 m. As can be seen, the two signals deviate. Part of this deviation is due to the travel-time difference of the direct signal and some of the difference is due to a different ghost effect for the finite-difference solution compared to the true solution. In effect the finite-difference signature is stretched compared to the true solution. The blue line is the result of a finite-difference simulation where the source is placed at the true depth using the optimized spatial delta functions. The fit is clearly improved compared to the simple source implementation approach using the nearest node.

There will also be an error in radiation pattern or amplitude versus radiation angle if the applied source depth do not coincide with the true source depth. This error is frequency dependent. In Fig. 3 the angle-dependent maximum amplitudes of the pressure field due to a source at depth 4 m are calculated analytically. These amplitudes are compared to the corresponding finite-difference calculated amplitudes. The finite-difference data is generated using the nearest node strategy, thus with an effective source depth of 10 m. The maximum amplitudes are normalized for the direct downgoing wave, which ensures that the amplitude error will zero when the radiation angle is zero. As can be seen, the errors increase with radiation angle and source frequency. We did similar calculations where we compared analytically calculated maximum

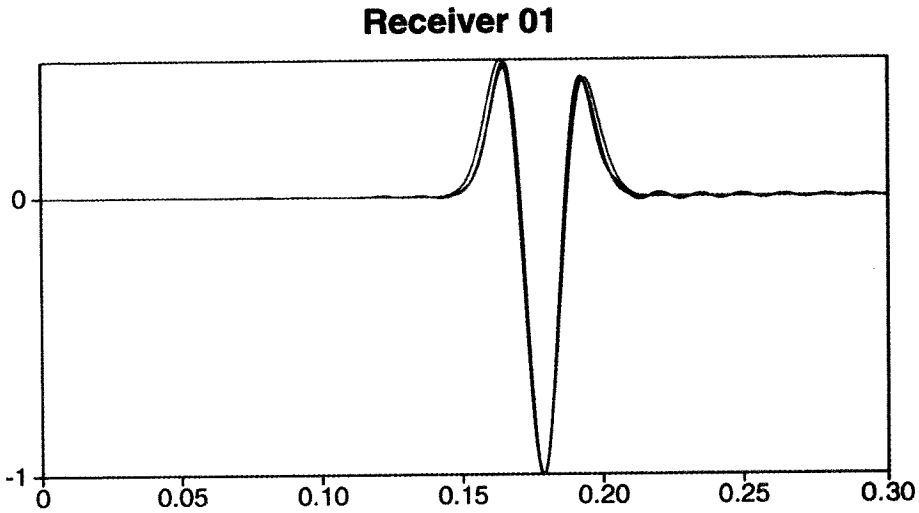

Fig. 1. Pressure at depth 100 m. Zero offset. Green line: analytical solution for source at 4 m. Blue line: finite-difference solution using phase-shift operators. Red line: finite-difference solution without phase-shift operators.

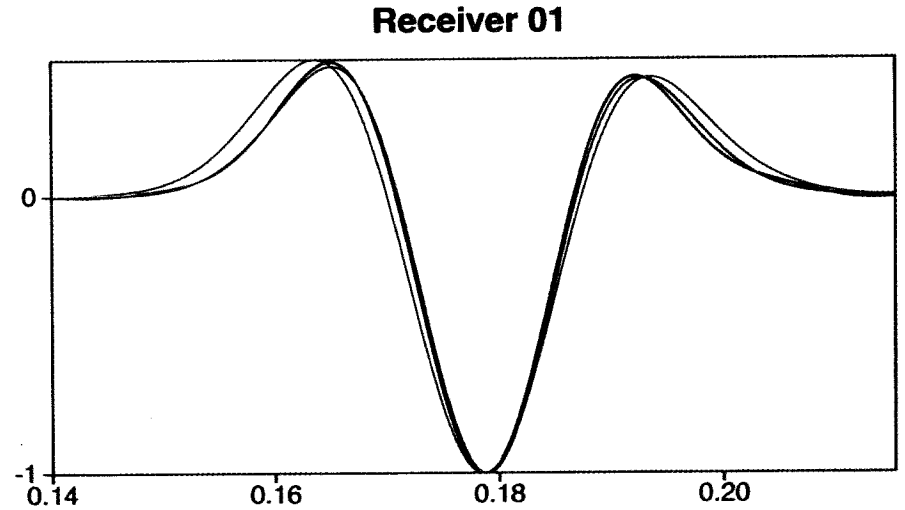

as in Fig. 3. This difference in radiation pattern is to be expected since the radiation pattern of a dipole depend on the distance between the "charges" and the "charge"-separation becomes more important with increased resolution (higher frequency). In Fig. 4 we compare the analytically calculated maximum amplitudes for a source at depth 4 m with finite-difference calculated maximum amplitudes using the operator strategy. As can be seen, the errors are drastically reduced and usually less than 1 percent.

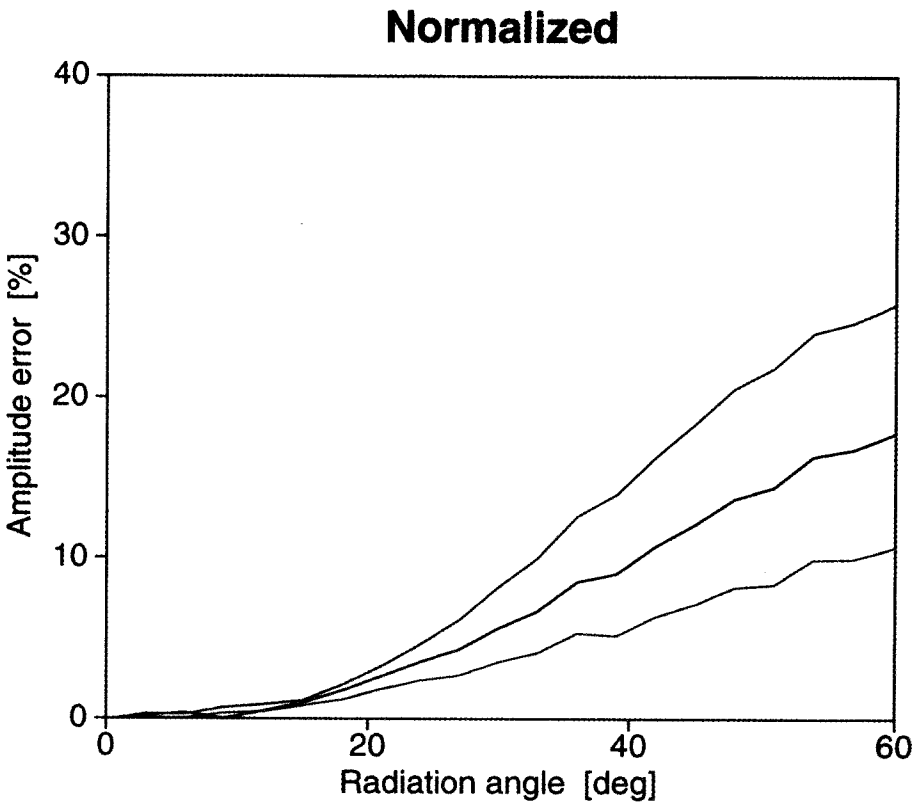

We have also performed a calculation for a realistic marine source array. The notional source signatures were generated with the Nucleus Marine Source Modeling module from PGS Seres. The 3090T array is shown in Fig. 5. All guns are at a depth of 5 m. The 3090T array contain 28 active guns. The corresponding notional source signatures are shown in Fig. 6.

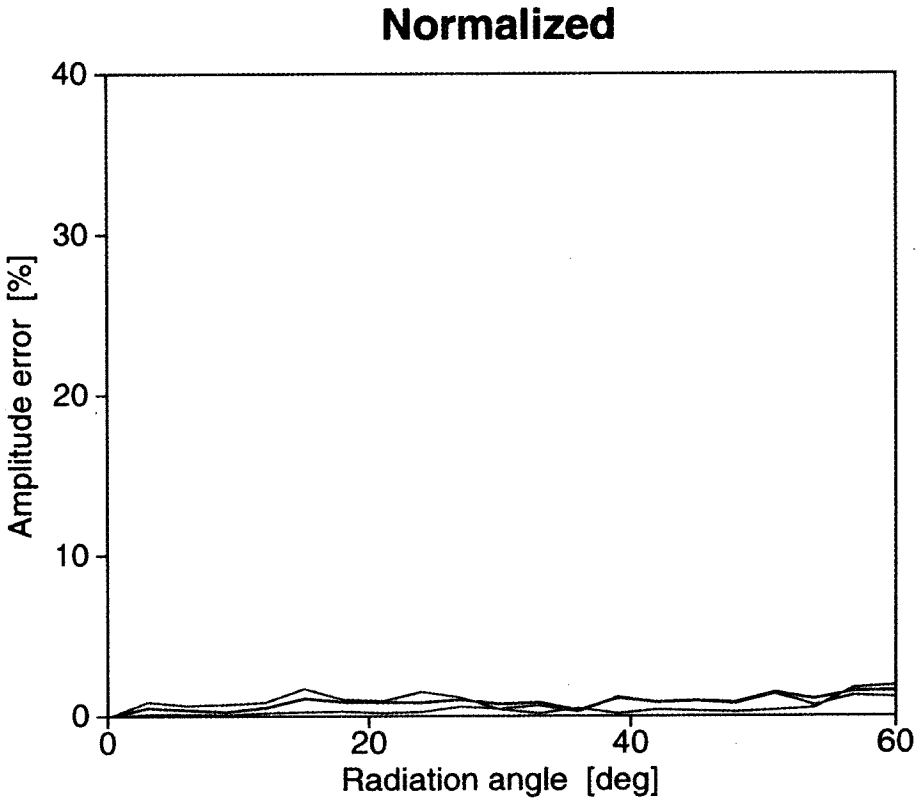

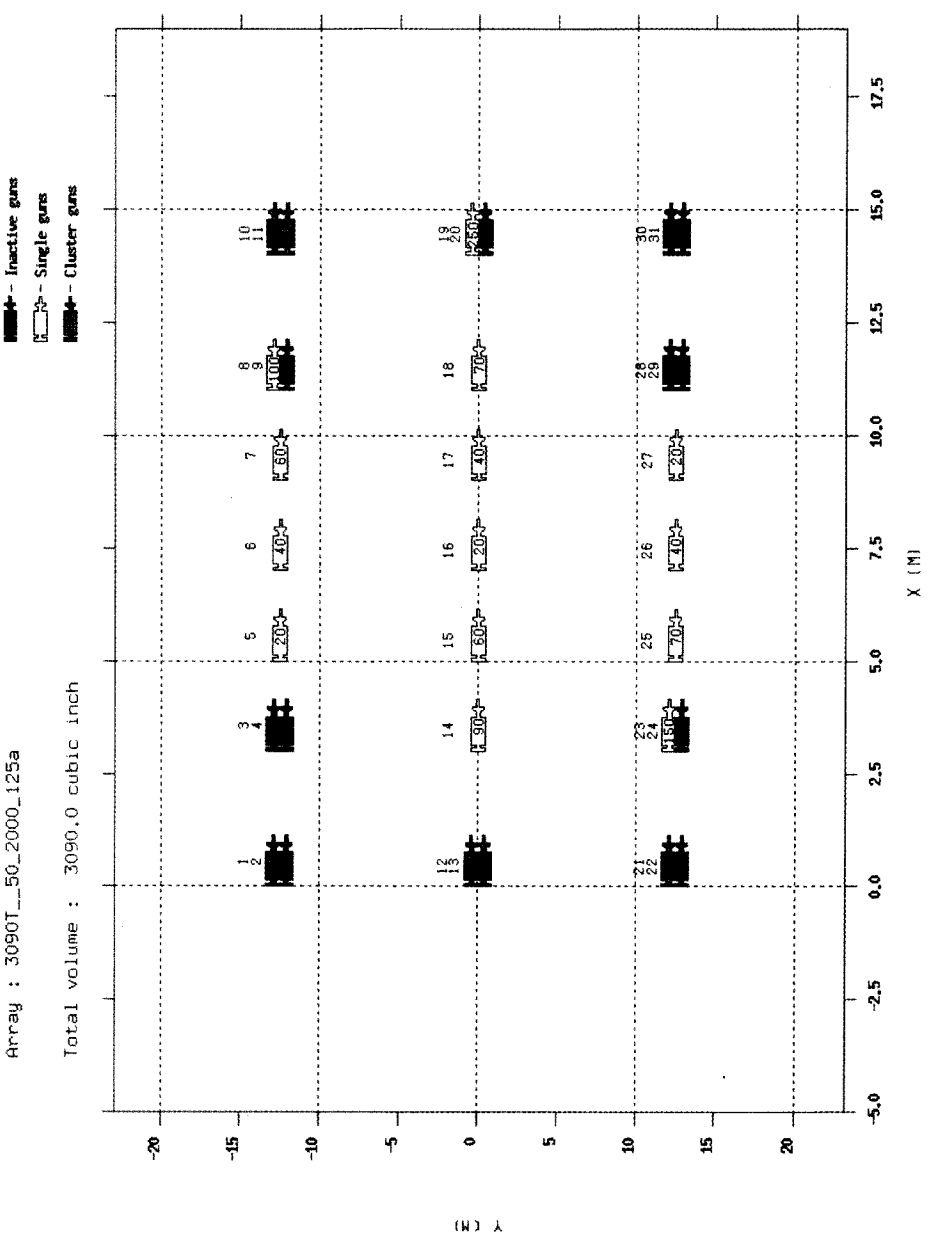
Array : 3090T__50_2000_125a
Total volume : 3090.0 cubic inch
Inactive guns
Single guns
Cluster guns
Y (M)
X (M)

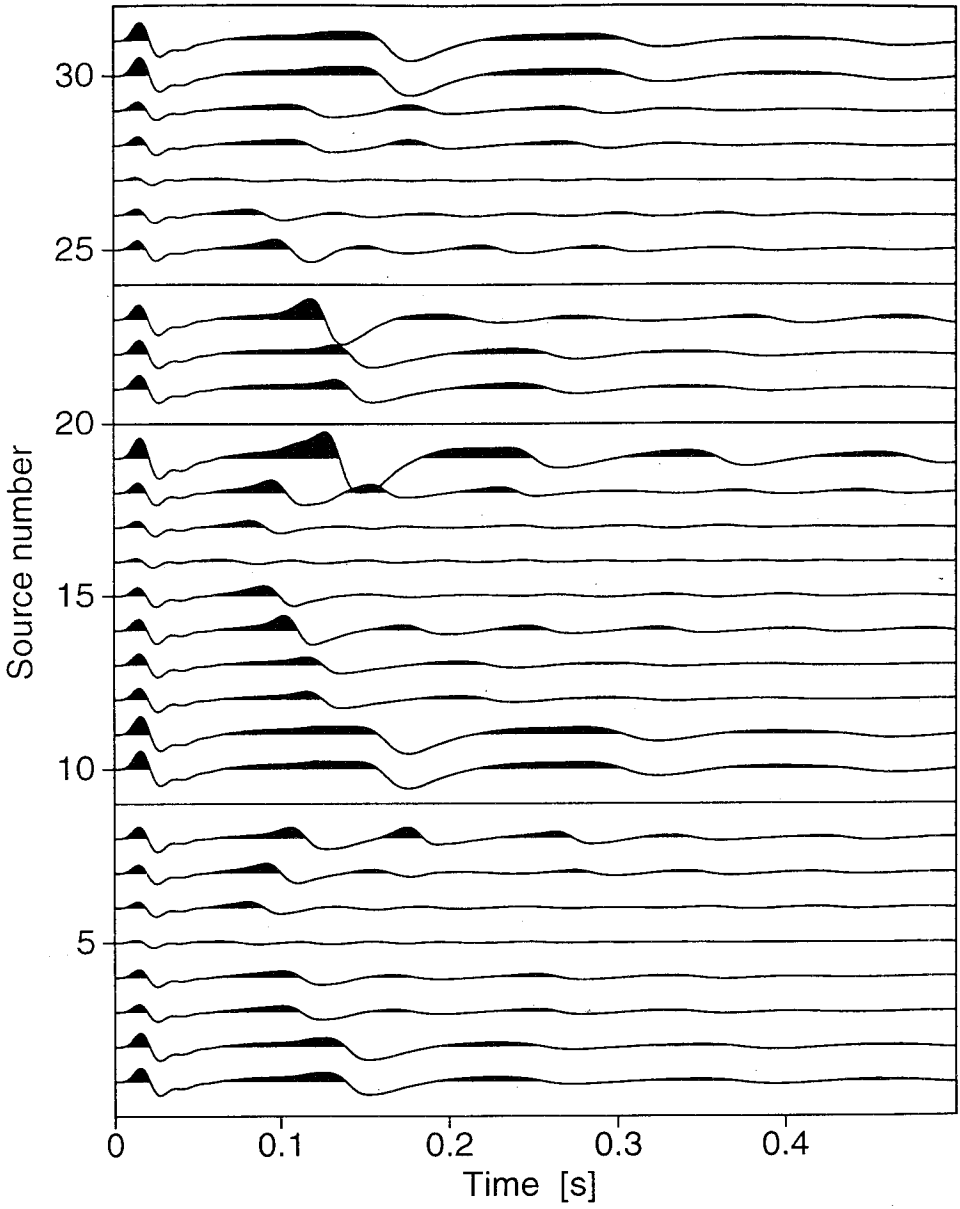
30
25
20
15
10
5
Source number
0
0.1
0.2
0.3
0.4
Time [s]

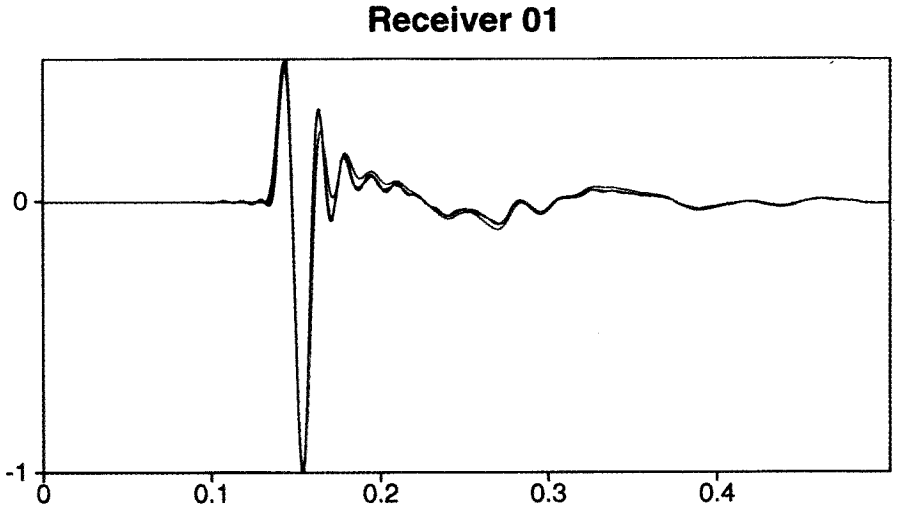

Fig. 7. Farfield signatures. Zero offset. Green line: analytical solution. Blue line: finite-difference solution using phase-shift operators. Red line: finite-difference solution without phase-shift operators.

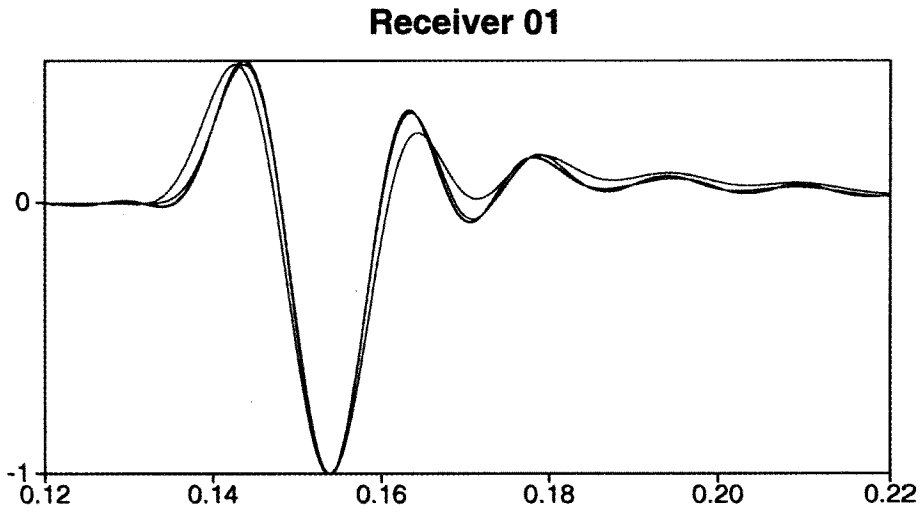

Fig. 8 shows a detail of Fig. 7 and both show farfield signatures calculated analytically and with finite differences. The analytical solution is plotted with a green line. The red line is the result of a finite-difference simulation where the optimized spatial delta functions are not used. This implies that all sources are located at the nearest node in the finite-difference simulation. Thus sources are in principle at erroneous positions in x-, y- and z-directions. Deviations can be seen in the arrival time and amplitude of the primary part of the signal and also to some extent for the more low frequent part related to the bubble oscillations. The blue line represent the result of a finite-difference simulation where the sources are placed at their true x-, y- and z-coordinates using the optimized spatial delta functions. The fit is clearly improved compared to the strategy of using the nearest nodes as the source positions.

The operators can also be used to allow for arbitrary receiver positions. Two acoustic 3D finite-difference shotgathers are modeled. The streamer is assumed to have a varying depth. The average depth is 10 m and the maximum deviations are $\pm$ 2 m. The deviations have a sinusoidal form with a wavelength of 500 m. The streamer length is 1000 m with nearest offset equal to 100 m. A cross section of the P-wave velocity model is shown in Fig. 9 and the resulting shotgather is shown in Fig. 10. The shotgather resulting from moving the recording positions to the nearest node in the finite-difference grid is shown in Fig. 11. The difference between the two shotgathers is shown in Fig. 12. All three shotgathers are scaled with time squared to compensate for the geometrical spreading effect and the overall scaling factor is identical for the three datasets. The sinusoidal depth variations of the streamer are clearly mirrored in the difference shotgather.

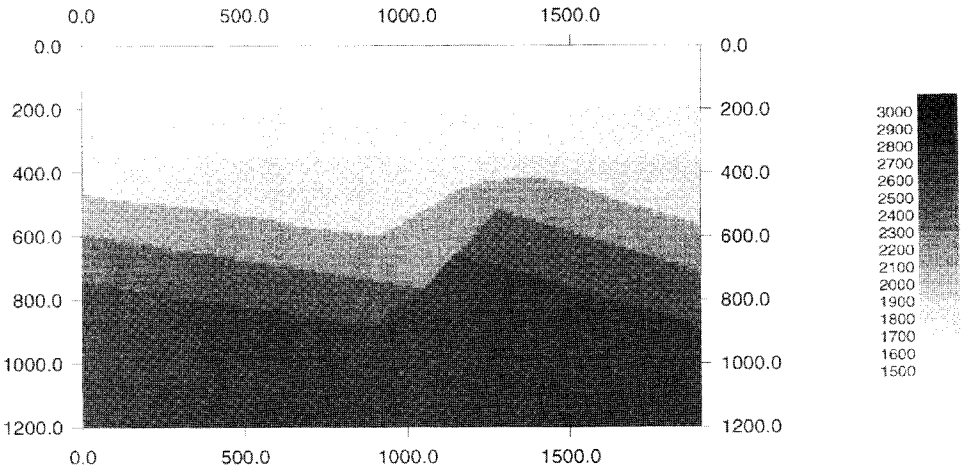

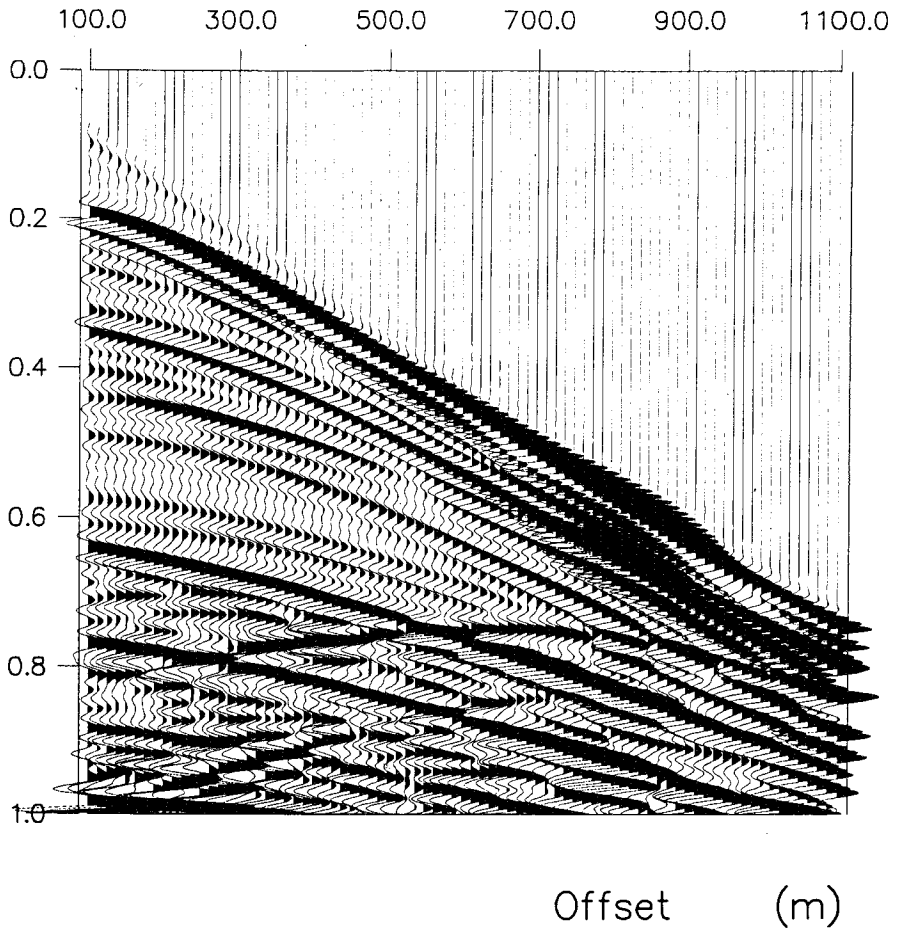

Fig. 10. Shotgather for receivers at true positions.

CONCLUSION

A method for positioning sources and receivers at arbitrary locations for coarse-grid finite-difference schemes has been presented. The method is based on designing optimized bandlimited approximations for both the Dirac delta function and the spatial derivative of the Dirac delta function. These operators can have a general phase shift which allows the operator to be centered

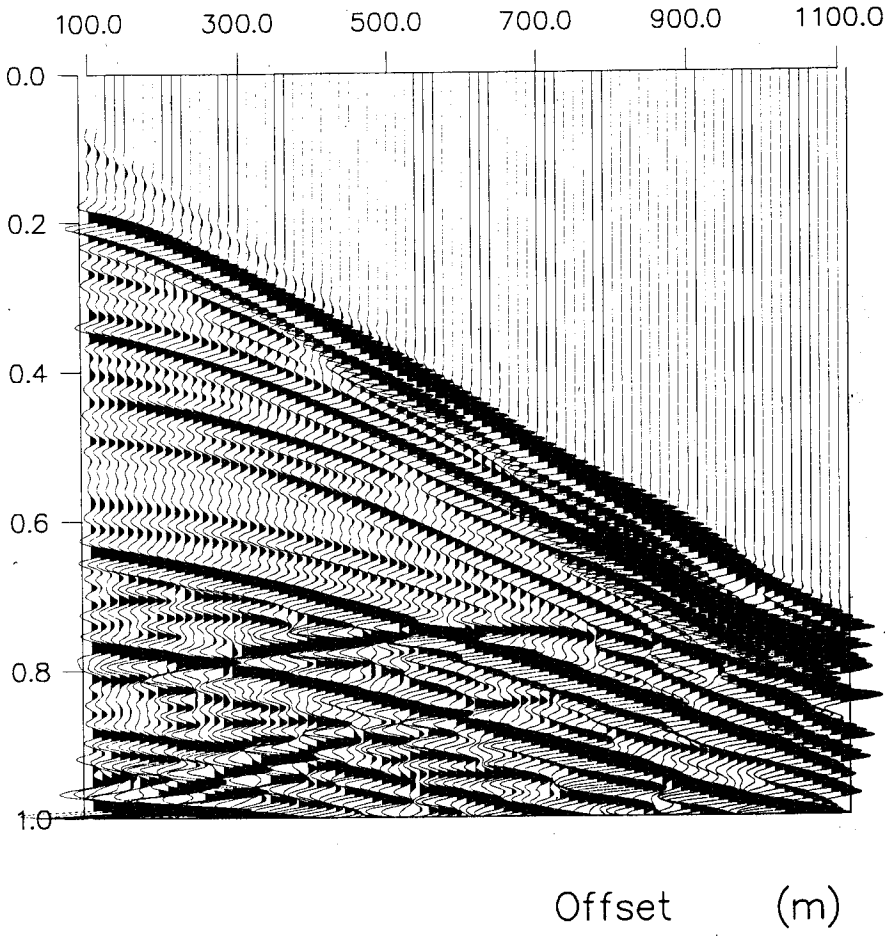

Fig. 11. Shotgather for receivers at nearest node in finite-difference grid.

function (monopole) used in the source term or Kirchhoff integral. The phase-shift derivative operator is identical to the spatially bandlimited derivative of the delta function (dipole) used in the source term or Kirchhoff integral. The acoustic and elastic Kirchhoff integral requires that proper approximations for the monopole and dipole source terms are known. Thus, these operators can increase the accuracy of reverse time migration schemes when the recorded field

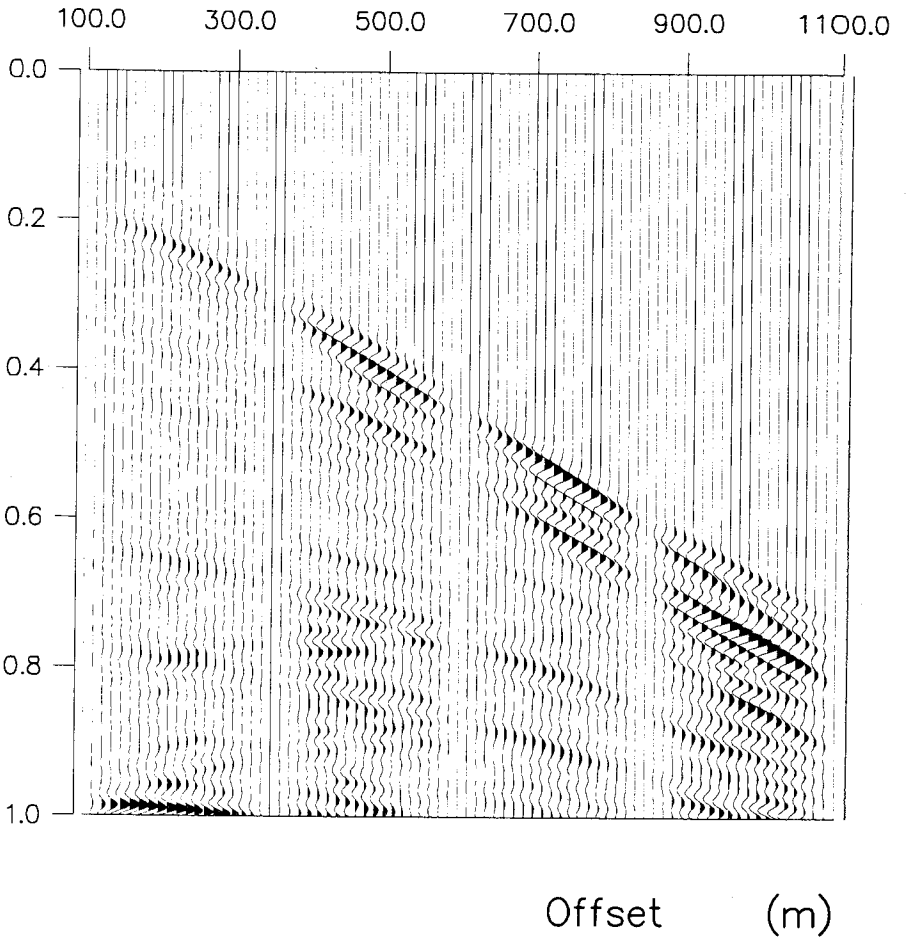

Fig. 12. Difference between shotgathers. Shotgather with receivers at true positions minus shotgather with receivers at nearest nodes.

The optimized phase-shift operators were tested both for a single source and a source array. Good agreement between the finite-difference solution and the analytical solution were found in both cases. Most important is that the error in amplitude versus radiation angle is drastically reduced using the optimized operator scheme.

A demonstration of the effect of variable streamer depths was also given. The operators where designed with a group velocity error criterion and the

ACKNOWLEDGMENTS

This work has been financially supported by the Statoil Research. We thank Statoil Research for the permission to publish this paper. We also wish to thank Hans J. Hoffmann of PGS Seres who has supplied the notional source signatures for the source array.

REFERENCES

Amundsen, L., 1993. Estimation of source array signatures. Geophysics, 58: 1865-1869.

Fornberg, B., 1975. On a Fourier method for the integration of hyperbolic equations. Soc. Ind. Appl. Math., J. Numer. Anal., 12: 509-528.

Holberg, O., 1987. Computational aspects of the choice of operator and sampling interval for numerical differentiation in large-scale simulation of wave phenomena. Geophys. Prosp., 37: 629-655.

Kosloff, D.D. and Baysal, E., 1982. Forward modeling by a Fourier method. Geophysics, 47: 1402-1412.

Landrø, M. and Sollie, R., 1992. Source signature determination by inversion. Geophysics, 57: 1633-1640.

Landrø, M., Mittet, R. and Sollie, R., 1993. Implementing measured source signatures in a coarse-grid, finite-difference modeling scheme. Geophysics, 58: 1852-1860.

Mittet, R., 1994. Implementation of the Kirchhoff integral for elastic waves in staggered-grid modeling schemes. Geophysics, 59: 1894-1901.

Mittet, R., Holberg, O., Arntsen, B. and Amundsen, L., 1988. Fast finite-difference modeling of 3-D elastic wave propagation. Expanded Abstr., 58th Ann. Internat. SEG Mtg., Anaheim: 1308-1311.

Reshef, M., Kosloff, D., Edwards, M. and Hsiung, C., 1988. Three-dimensional acoustic modelling by the Fourier method. Geophysics, 53: 1175-1183.

Zhu, J. and Lines, L.R., 1997. Implicit interpolation in reverse-time migration. Geophysics, 62: 906-917.

Ziolkowski, A., Parkes, G. and Haugland, T., 1982. The signature of an air gun array: Computation from near-field measurements including interactions. Geophysics, 47: 1413-1421.

APPENDIX A

Dipole and derivative operator

The dipole operator needed in the source term of the wave equation or in the implementation of the boundary condition is the derivative of the Dirac delta function

$$\partial_x \delta(x - x_s) \quad . \tag{A-1}$$

$$\partial_x\phi(x + \delta x) = \int_{-\infty}^{\infty} dx'\{-\partial_x'\delta(x' - \delta x)\}\phi(x + x') = d_x^{\delta x} * \phi(x) \ . \quad \text{(A-2)}$$

Assume that this operator can be bandlimited and is to be used on a regularly sampled function with sampling interval Δx. Let $x = i\Delta x$ with i integer. Let $\delta x = \eta\Delta x$ with η a real number such that $-0.5 \leq \eta \leq 0.5$. The two special cases $\eta = -0.5$ and $\eta = 0.5$ will be the forward and backward derivative operators given by Holberg (1987). The discretized version of $d_x^{\delta x}$ is denoted D_x^{η} and the bandlimited Dirac delta function is denoted $\tilde{\delta}$,

$$\begin{aligned}\partial_x\phi(j\Delta x + \eta\Delta x) &= D_x^{\eta}\phi(j\Delta x) \\ &= \sum_{l=-L}^{L} \Delta x[-\partial_x\tilde{\delta}(l\Delta x - \eta\Delta x)]\phi(j\Delta x + l\Delta x) \\ &= \sum_{l=-L}^{L} \alpha_l^{\eta}\phi_{j+l} \ . \end{aligned} \quad \text{(A-3)}$$

The Fourier response of D_x^{η} is,

$$D^{\eta}(k) = (1/\Delta x)\sum_{l=-L}^{L} \alpha_l^{\eta} e^{ik(l-\eta)\Delta x} \ . \quad \text{(A-4)}$$

Let the response $D^{\eta}(k)$ be represented by

$$D^{\eta}(k) = ik[1 + \epsilon^{\eta}(k)] \ , \quad \text{(A-5)}$$

where $\epsilon^{\eta}(k)$ is the relative error in frequency response of the operator D_x^{η}. The derivative of the frequency response of $D^{\eta}(k)$ is

$$\partial_k D^{\eta}(k) = i[1 + \epsilon^{\eta}(k) + k\partial_k\epsilon^{\eta}(k)] \ . \quad \text{(A-6)}$$

If it is required that $D^{\eta}(k)$ should be as close to ik as possible then,

$$\min[D^{\eta}(k) - ik] = \min[\epsilon^{\eta}(k)] \ . \quad \text{(A-7)}$$

If it is required that the derivative of $D^{\eta}(k)$ with respect to k should be as close to i as possible then,

$$\min[(1/i)\partial_k D^{\eta}(k) - 1] = \min[\epsilon^{\eta}(k) + k\partial_k\epsilon^{\eta}(k)] \ , \quad \text{(A-8)}$$

which will make the operator response $D^{\eta}(k)$ close to ik and close to equiripple simultaneously. This error criterion is identical to the group-velocity criterion introduced by Holberg (1987).

The chosen procedure is to minimize the error functional ϵ_L^η,

$$\epsilon_L^\eta = [\int_{k=0}^{K_m} dk\{(1/i)\partial_k D^\eta(k) - 1\}^n + w(\sum_{l=-L}^{L} \alpha_l^\eta)]^2 \quad , \tag{A-10}$$

where

$$(1/i)\partial_k D^\eta(k) = \sum_{l=-L}^{L} \alpha_l^\eta (l - \eta) e^{ik(l-\eta)\Delta x} \quad . \tag{A-11}$$

The term proportional to the weight w in equation (A-10) ensures that the sum of all derivative operator coefficients is zero. This constraint must be implemented to give operators, which when applied to constant functions give a derivative of zero as result, independently of the phase shift. The best w value was found to be typically 5×10^{-3} and the best value of n was found to be 4. An additional constraint is that the relative group velocity error $\epsilon_{gr}^\eta(k)$ is less than the tolerance E_m for all wavenumbers up to the maximum wavenumber K_m. The coefficients α_l^η are the variables in this standard least square problem. A solution is accepted when K_m can not be increased further with the given E_m. The value of E_m is of order 10^{-2} - 10^{-3}. For the numerical examples in this paper the maximum error in group velocity is 0.001.

APPENDIX B

Monopole and interpolation operator

The monopole operator needed in the source term of the wave equation or in the implementation of the boundary condition is the Dirac delta function,

$$\delta(x - x_s) \quad . \tag{B-1}$$

The Dirac delta function also defines the convolutional interpolation operator $b_x^{\delta x}$,

$$\phi(x + \delta x) = \int_{-\infty}^{\infty} dx'\{\delta(x' - \delta x)\}\phi(x + x') = b_x^{\delta x} * \phi(x) \quad . \tag{B-2}$$

Assume that this operator can be bandlimited and is to be used on a regularly sampled function with sampling interval Δx. Let $x = i\Delta x$ with i integer. Let $\delta x = \eta\Delta x$ with η real number such that $-0.5 \leq \eta \leq 0.5$. The discretized version of $b_x^{\delta x}$ is denoted B_x^η,

$$= \sum_{l=-L}^{L} \Delta x[\tilde{\delta}(l\Delta x - \eta\Delta x)]\phi(j\Delta x + l\Delta x)$$

$$= \sum_{l=-L}^{L} \beta_l^{\eta}\phi_{j+l} \quad . \tag{B-3}$$

The Fourier response of B_x^{η} is

$$B^{\eta}(k) = \sum_{l=-L}^{L} \beta_l^{\eta}\, e^{ik(l-\eta)\Delta x} \quad . \tag{B-4}$$

Let the response of $B^{\eta}(k)$ be represented by

$$B^{\eta}(k) = 1 + \epsilon^{\eta}(k) \quad , \tag{B-5}$$

where $\epsilon^{\eta}(k)$ is the relative error in frequency response of the operator B_x^{η}. The derivative of the frequency response of $B^{\eta}(k)$ is

$$\partial_k B^{\eta}(k) = \partial_k \epsilon^{\eta}(k) \quad . \tag{B-6}$$

The group velocity criterion can be used for the interpolation operator as for the derivative operator discussed in Appendix A. If it is required that $B^{\eta}(k)$ is as close as possible to 1 and that the derivative of $B^{\eta}(k)$ with respect to k is as close to 0 as possible then,

$$\min[B^{\eta}(k) - 1 + k\partial_k B^{\eta}(k)] = \min[\epsilon^{\eta}(k) + k\partial_k \epsilon^{\eta}(k)] = \min[\epsilon_{gr}^{\eta}(k)] \quad , \tag{B-7}$$

which will make the operator response $B^{\eta}(k)$ close to equiripple.

The error functional ϵ_L^{η} is then,

$$\epsilon_L^{\eta} = [\int_{k=0}^{K_m} dk\{B^{\eta}(k) - 1 + k\partial_k B^{\eta}(k)\}^n + w(\sum_{l=-L}^{L} \beta_l^{\eta} - 1)]^2 \quad , \tag{B-8}$$

where

$$B^{\eta}(k) - 1 + k\partial_k B^{\eta}(k) = \sum_{l=-L}^{L} \{\beta_l^{\eta}[1 + ik(l-\eta)\Delta x]e^{ik(l-\eta)\Delta x}\} - 1 \quad . \tag{B-9}$$

The term proportional to w in equation (B-8) ensures that the sum of all interpolation operator coefficients is equal to 1. This constraint must be implemented to give operators, which when applied to a constant function give the constant function as result independently of phase shift. The optimized coefficients β_l^{η} are found with the same least square procedure as the optimized α_l^{η} coefficients discussed in Appendix A.